Supporting information for: Dipole-induced Asymmetric Conduction in Tunneling Junctions Comprising Self-assembled Monolayers

Andrii Kovalchuk,[†] David A. Egger,[‡] Tarek Abu-Husein,[¶] Egbert Zojer,[§] Andreas Terfort,[¶] and Ryan C. Chiechi[*,†]

†*Stratingh Institute for Chemistry & Zernike Institute for Advanced Materials, University of Groningen, Nijenborgh 4, 9747 AG Groningen, The Netherlands*

‡*Department of Materials and Interfaces, Weizmann Institute of Science, Rehovoth 76100, Israel*

¶*Institut für Anorganische und Analytische Chemie, Universität Frankfurt, Max-von-Laue-Straße 7, 60438 Frankfurt, Germany*

§*Institute of Solid State Physics, NAWI Graz, Graz University of Technology, Graz, Austria*

E-mail: r.c.chiechi@rug.nl

Experimental

Sample preparation

The Au substrates were prepared by mechanical Template Stripping (TS) as described elsewhere.[S1] We deposited 100 nm of Au (99.99%) by thermal vacuum deposition onto a 3" Silicon wafer (with no adhesion layer). Using UV-curable Optical Adhesive (OA) Norland 61, 1 cm^2 glass chips are glued on the metal surface. All samples were prepared following the procedure from Ref. S2. In brief: freshly cleaved gold slides were incubated in 1 mM solutions in ethanol at room temperature for $\sim$ 24h. Prior to making a solution ethanol was degassed by bubbling nitrogen gas through for at least 20 minutes and all solutions were kept under nitrogen atmosphere to prevent undesirable oxidation of thiol anchoring group. All compounds were synthesized and purified according to Ref. S2.

Data acqusition and analysis

Data were acquired in a home-built setup that is described in detail elsewhere.[S3] Samples were taken out from solution, carefully rinsed with pure ethanol and gently dried with nitrogen. Each SAM was then measured by placing a sharp tip of EGaIn in visual contact with the surface and acquiring at least 1000 scans across 10 substrates. The traces in which the instrument reached compliance were considered short circuits and were discarded (they reflect only the compliance limit of the instrument and have no physical meaning). TP1-up showed lower solubility than and TP1-down and showed signs of partial precipitation onto the gold surface leading to the appearance of traces where values of J were systematically *ca.* two of orders of magnitude lower than the geometric mean. These traces, which were present only in TP1-up data and made up a small fraction of the total traces, most likely reflect junctions comprising multilayers and were discarded.

Histograms of the values of J at each value of V were then fit to Gaussian distributions. The standard deviation of a fit (σ) was then recalculated into 95% confidence interval using

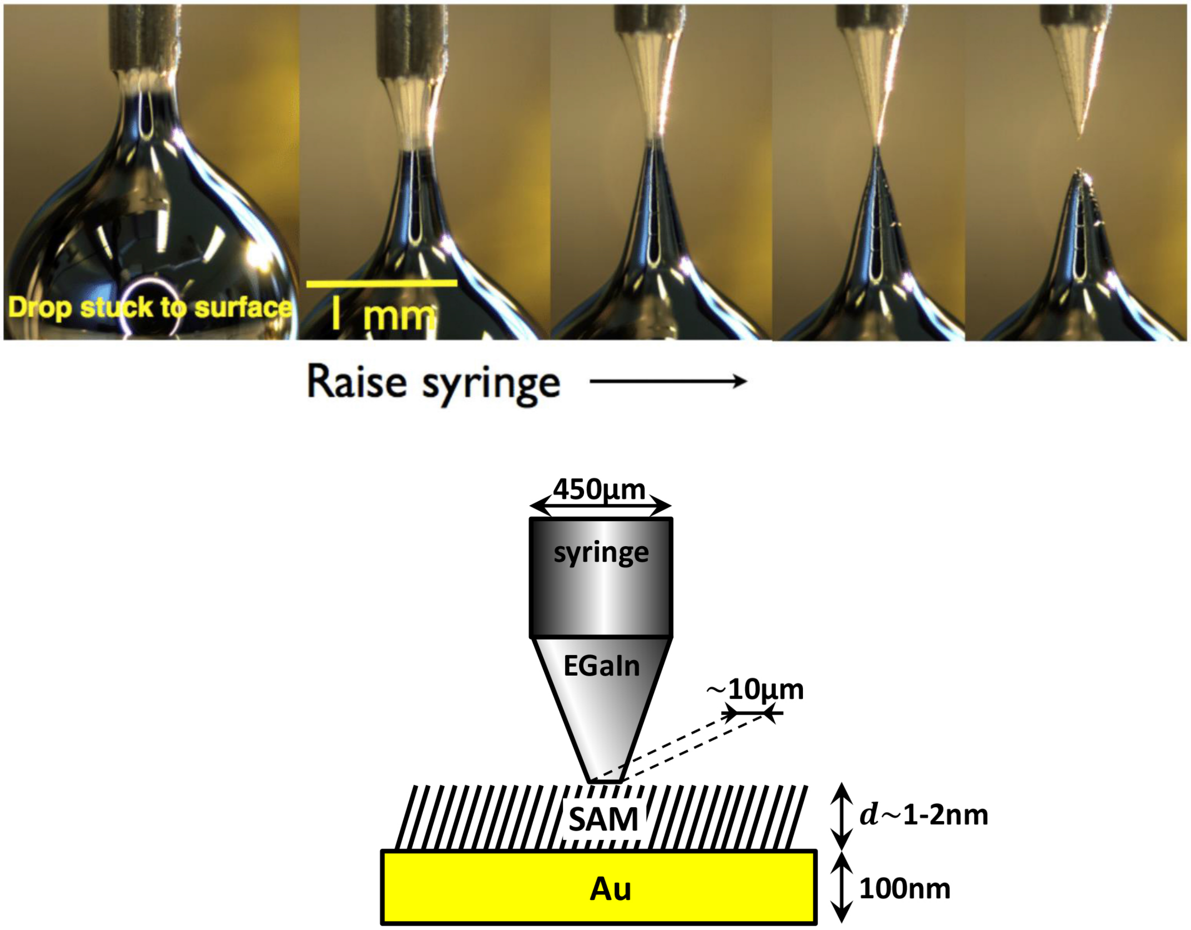

Figure S1: Photographs of the tip formation and a schematic of an assembled EGaIn junction.

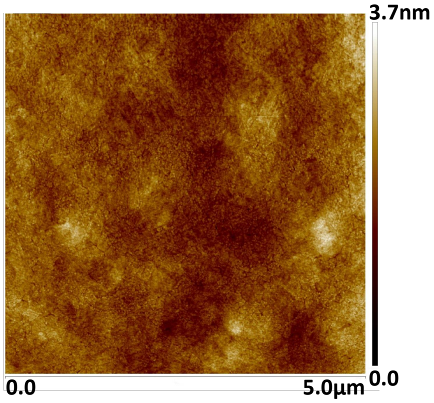

Figure S2: AFM image of a pristine $\mathrm{Au}^{\mathrm{TS}}$ substrate with RMS roughness of 0.249 nm.

following equation $\mathrm{CI} = t\frac{\sigma}{\sqrt{N}}$, where t is the coefficient in t-distribution and N is the number of degrees of freedom for our system ($N_{junctions} - 1$). The same procedure was applied to calculate asymmetry parameter (*log* χ).

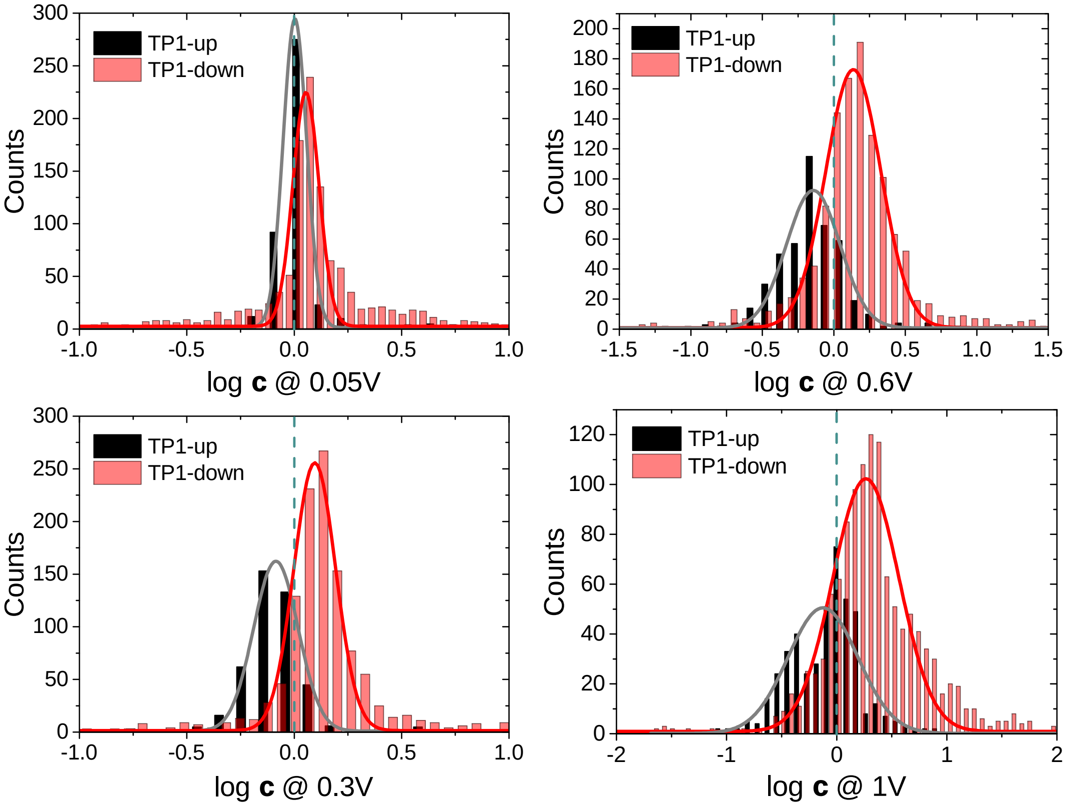

Figure S3: Exemplary histograms of *log* χ at different voltages along with Gaussian fits.

In order to analyze statistical significance of an effect in J/V and χ data we carried out a Welch's t-test to compute the p-value comparing histograms of *log* $|J|$ and *log* χ for TP1-up and TP1-down at each voltage step. A p-value, in this instance, is a measure of the probability of the difference in the mean values of the two histograms being due to random chance *i.e.*, with what statistical certainty we can claim that the dipole moment is affecting J or χ. Low p-values mean that the null hypothesis is likely to be false, *i.e.*, an effect is unlikely to be due to random chance. In the main text the χ plot has 95% CI as error bars simply by convention, such that our plots are easily comparable to the literature. However, all values of χ past 0.2 V also pass the much more rigorous 99.9% confidence test. Thus, we can state with 99.9% statistical certainty that J differs at positive bias and that χ differs almost everywhere and that the difference is not due to random fluctuations.

In recent years a lot of controversy has arisen regarding the misuse of p-values and the lack of reproducibility and replicability of certain results based on the p-value statistics. Recently American Statistical Association (ASA) issued a Statement on Statistical Significance and P-values[S4] to clarify several widely agreed upon principles underlying the proper use and interpretation of the p-value. We are duly aware of the pitfalls of p-values and do not base our conclusions solely on the results of a t-test. Rather, we (correctly) use these statistical tests to support the differences that are present in Fig. S3 and to present such statistical data mathematically instead of subjectively, by showing each histogram separately. We also use a methodology that emphasizes estimation over testing (confidence intervals) and the results of both are in good agreement.

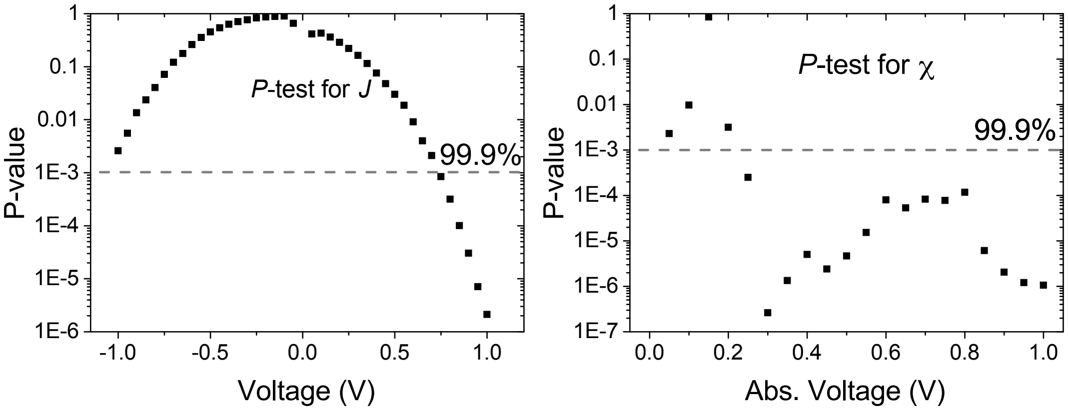

Figure S4: Determination of statistical significance of an effect between SAMs of TP1-up and TP1-down using a p-test in current density (J, on the left) and asymmetry (χ, on the right) parameters. Dashed line corresponds to the chosen confidence level of 99.9%. The p-test for J shows that the null hypothesis can be rejected with a high degree of certainty for high positive bias, *i.e.*, the statistical certainty of the difference in distributions of J being due to an experimental effect and not random chance is $> 99.9\%$. For χ all values past 0.2 V show statistical significance of the effect.

DFT calculations

Single-molecule transport simulations

We calculated the zero-bias transmission probability for TP1-up and TP1-down in single-molecule junctions using DFT[S5] to probe the electronic effects of the molecule/electrode complex on transport. We simulated single-molecule junctions using 11- and 12-atom clusters

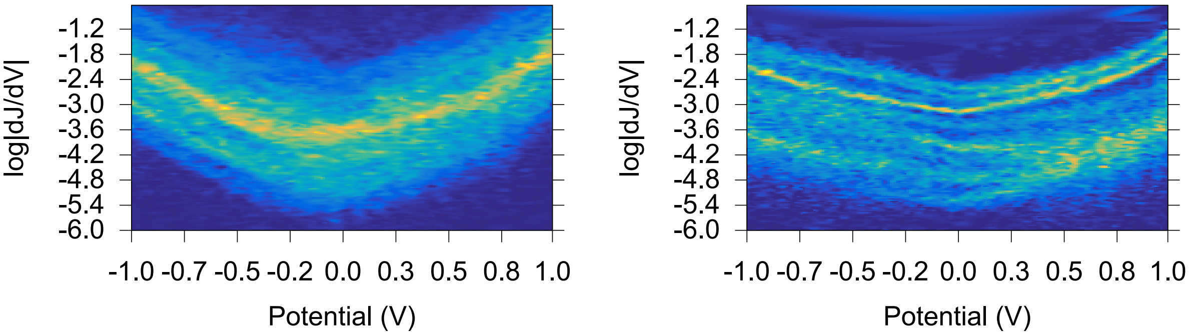

Figure S5: Conductance heatmap plots for TP1-down (left) and TP1-up (right) showing histograms binned to $log|\frac{dJ}{dV}|$ (conductance, Y-axis) versus potential (in V, X-axis). The colors correspond to the frequencies of the histograms; lighter colors indicate higher frequencies. The bowl-shaped conductance is indicative of non-resonant tunneling and roughly reproduces the bowl shape of the calculated zero-bias transmission curve shown in the Fig. S6.

of Au(111) as electrodes. The "bottom" electrode is coupled through a S-Au bond at a FCC hollow site and the "top" electrode is physisorbed; all angles and distances are conserved. The DOS and transmission curves were calculated with Gaussian 09 using B3LYP/LANL2DZ in accordance with literature procedures.[S6] We computed gas-phase orbital energies with Gaussian 09 using HSE06/6-311g*. The frontier orbitals from these calculations are shown in Fig. S7. The resulting transmission spectra, shown in Fig. S6, overlap almost completely with only a slight—and insignificant—offset in magnitude. Thus, single-molecule transmission calculations do not predict any difference in the conductance of TP1-up and TP1-down nor any difference in the frontier orbitals. Thus, the mechanism of asymmetry is likely due to a collective effect that is present in SAM-junctions, but absent in single-molecule junctions.

The model used in these single-molecule calculations is not aimed at predicting the properties of the actual junction, but to test the hypothesis that the effects seen in J/V curves are due to shifts that take place in the assembled monolayer by comparing individual molecules *in silico*. These calculations are sensitive only to the electronic structure of the molecule-electrode complex and will not reflect effects from applied fields or the electrostatics arising from collective effects in a monolayer. If the effect is indeed from the collective action of dipoles (regardless of the exact mechanism), it should *not* be present in the calculated

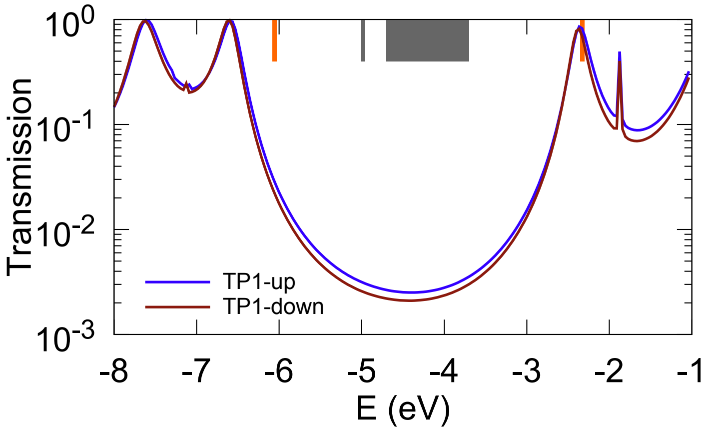

Figure S6: Calculated zero-bias transmission probabilities for TP1-up (blue) and TP1-down (red) single-molecule junctions plotted against energy (eV). The molecules are bound to FCC hollow sites on Au(111) electrodes in their minimized geometries using identical Au-S lengths and angles. The top Au(111) contacts are physisorbed at equal lengths and angles. The gas-phase HOMO and LUMO are marked with orange bars along the top at -6.03 and -2.35 eV respectively. The thin grey bar shows the uncorrected Fermi energy $E_f = -4.96$ eV and the thick grey bar estimates the range of E_f for EGaIn.

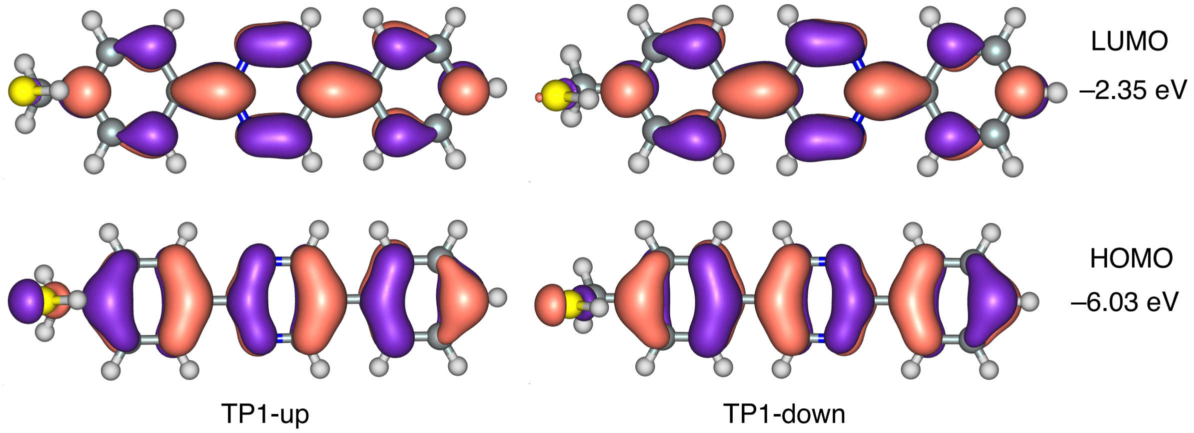

Figure S7: Visualizations of the frontier orbtials of TP1-up and TP1-down showing subtle differences in the symmetries, particularly near the pyrimidyl rings.

Au/molecule//Au model junctions.

Simulations employing periodic boundary conditions

The substrate-SAM interfaces and free-standing SAMs were modelled using a $(\sqrt{3} \times 3)$ surface unit-cell containing two molecules in herringbone arrangement as in our previous work.[S2] For the isolated molecule calculations the unit cells vectors were doubled 3 times in

x- and 2 times in y-direction. In all calculations without a metal surface, the molecules were capped with hydrogen atoms. Our density functional theory calculations were performed with the plane-wave VASP code[S7] applying the HSE screened hybrid functional[S8,S9] and an $8 \times 5 \times 1$ k-grid for the laterally periodic systems. In all our calculations, a dipole correction was used. The external electric fields were applied fully self-consistently in our VASP calculations, using the EFIELD tag. In these calculations, we used the wavefunctions of the field-free calculations as a starting guess for the self-consistent field procedures. The use of a hybrid functional for calculating the electronic states in the here considered SAMs and molecules is important to ensure a reliable ordering of the electronic states bearing in mind the different self-interaction errors associated with σ- and π-states among the high-lying occupied orbitals in pyrimidines.[S10] Nevertheless, when calculating the molecular orbital densities of the isolated molecules and free-standing SAMs, in some cases a localized state was found to be the HOMO even with the HSE functional, and the delocalized π-orbital was deeper in energy. As only reasonably delocalized orbitals represent relevant transport channels, we analyzed the charge density associated with the highest-lying delocalized orbital, *i.e.*, the highest occupied π-state (HOPS), in all cases.

The average field within the TP1-up SAM, for an external field of -0.1 eV/Å, was determined in the following way: the potential step in vacuum to generate the electric field for the free-standing SAM was $+2.3$ eV. Note that this includes not only the external field present in the calculation, but also the -1.0 eV drop in energy due to the polar monolayer, which we determined self-consistently in a calculation of the free-standing SAM under field-free conditions. Our unit cell in the calculations was 48 Å long, and the thickness of the TP1-up SAM is 18.2 Å. It follows that the total potential drop over the SAM amounts to 0.32 eV, yielding an internal field of 0.018 eV/Å. Using the ratio of the external and internal fields, we find that the effective dielectric constant of the SAM is 5.6. We can then determine the total potential drop over a junction in which an average field of 0.018 eV/Å is present in the SAM: as the perpendicular component of the electric displacement field remains constant at the SAM/Ga_2O_3 interface, we obtain for the field within the oxide a value of $E_{Ga_2O_3} = E_{SAM} \times \epsilon_{SAM}/\epsilon_{Ga_2O_3} = 0.01$ eV/Å. Consequently, the total potential drop including a 7 Å thick dielectric amounts to 0.39 V.

References

(S1) Weiss, E. A.; Kaufman, G. K.; Kriebel, J. K.; Li, Z.; Schalek, R.; Whitesides, G. M. Si/SiO_2-Templated Formation of Ultraflat Metal Surfaces on Glass, Polymer, and Solder Supports: Their Use as Substrates for Self-Assembled Monolayers. *Langmuir* **2007**, *23*, 9686–9694.

(S2) Abu-Husein, T.; Schuster, S.; Egger, D. A.; Kind, M.; Santowski, T.; Wiesner, A.; Chiechi, R.; Zojer, E.; Terfort, A.; Zharnikov, M. The Effects of Embedded Dipoles in Aromatic Self-Assembled Monolayers. *Adv. Func. Mater.* **2015**, *25*, 3943–3957.

(S3) Fracasso, D.; Valkenier, H.; Hummelen, J. C.; Solomon, G. C.; Chiechi, R. C. Evidence for Quantum Interference in SAMs of Arylethynylene Thiolates in Tunneling Junctions with Eutectic Ga-In (EGaIn) Top-Contacts. *J. Am. Chem. Soc.* **2011**, *133*, 9556–9563.

(S4) Wasserstein, R. L.; Lazar, N. A. The ASA's statement on p-values: context, process, and purpose. *The American Statistician*

(S5) Obersteiner, V.; Egger, D. A.; Zojer, E. Impact of Anchoring Groups on Ballistic Transport: Single Molecule vs Monolayer Junctions. *J. Phys. Chem. C* **2015**, *119*, 21198–21208.

(S6) Herrmann, C.; Solomon, G. C.; Subotnik, J. E.; Mujica, V.; Ratner, M. A. Ghost transmission: How large basis sets can make electron transport calculations worse. *J. Chem. Phys.* **2010**, *132*, 024103.

(S7) Kresse, G.; Furthmüller, J. Efficient iterative schemes for *ab initio* total-energy calculations using a plane-wave basis set. *Phys. Rev. B* **1996**, *54*, 11169–11186.

(S8) Heyd, J.; Scuseria, G. E.; Ernzerhof, M. Hybrid functionals based on a screened Coulomb potential. *J. Chem. Phys.* **2003**, *118*, 8207–8215.

(S9) Heyd, J.; Scuseria, G. E.; Ernzerhof, M. Erratum: “Hybrid functionals based on a screened Coulomb potential” [J. Chem. Phys.118, 8207 (2003)]. *J. Chem. Phys.* **2006**, *124*, 219906.

(S10) Rissner, F.; Egger, D. A.; Natan, A.; Körzdörfer, T.; Kümmel, S.; Kronik, L.; Zojer, E. Collectively Induced Quantum-Confined Stark Effect in Monolayers of Molecules Consisting of Polar Repeating Units. *J. Am. Chem. Soc.* **2011**, *133*, 18634–18645.